J. Tokyo Med. Univ., **66**(2) : 188-195, 2008

Diffusion-weighted imaging in the orbital region : Comparison of coronal images by direct imaging and multiplanar reconstruction

Fumio KOTAKE, Keiji MORIMOTO, Taizou OZUKI, Gen ARAI

Department of Radiology, Tokyo Medical University, Kasumigaura Hospital

Abstract

Strong susceptibility artifacts occur in diffusion-weighted imaging (DWI) of the orbital region because of the presence of air in the maxillary sinus on the lower side. Therefore, the direct coronal images have not been used for diagnoses. In the present study, coronal images were prepared by multiplanar reconstruction (MPR) for magnetic resonance imaging (MRI) phantoms, handmade phantoms, and normal volunteers. MPR-coronal images were compared with direct coronal images and their clinical utility was verified.

In the MRI phantom experiment under strong effects of susceptibility artifacts, the distortion rate of the direct coronal DWI was −23.2%. In contrast, the distortion rate of the MPR-coronal DWI was within the allowable range of 1.1%. In the handmade phantom experiment with little effect of susceptibility artifact, there was no significant difference in the apparent diffusion coefficient (ADC) value between the direct coronal DWI and MPR-coronal DWI. Therefore, it was considered that the MPR-coronal ADC map could be used for measuring the ADC value. The average signal-to-noise ratio (SNR) of the globes of volunteers was 1.90±0.25 (mean±standard deviation) for direct coronal DWI and 1.78±0.25 for MPR-coronal DWI. There was no significant difference ($P=0.092$). The average SNR of the white matter of the frontal lobe was 2.29±0.34 for direct coronal DWI and 2.30±0.27 for MPR-coronal DWI with no significant difference ($P=0.878$).

MPR-coronal DWI (monochrome reverse imaging) was performed on cases of optic neuritis, orbital malignant lymphoma, and dysthyroid ophthalmopathy. As a result, images with no distortion were obtained and lesions were visualized as areas of significant high signal intensity.

The above test results and clinical investigation for orbital disorders suggest that MPR-coronal DWI provides better images than direct coronal DWI in the orbital region. It could be used for clinical cases because it does not involve any problems in ADC measurements and SNR.

Introduction

The orbit is a small region with many organs. Therefore, diagnostic imaging using only a transverse image with magnetic resonance imaging (MRI) is insufficient. Coronal images and sagittal images are required. In particular, since the diameter of the optic nerve is approximately only 3 mm, no precise signal can be obtained due to the partial volume effect when visualized in transverse images. Therefore, the coronal image is indispensable. The usefulness of diffusion-weighted imaging (DWI) is widely recognized for the

Received September 20, 2007, Accepted November 12, 2007

Key words : Orbit, Magnetic resonance imaging, Diffusion-weighted imaging, Multiplanar reconstruction, Isotropic imaging

Corresponding author : Fumio KOTAKE, Department of Radiology, Tokyo Medical University, Kasumigaura Hospital, 3-20-1 Ami-machi chuo, Inashikigun, Ibaraki 300-0395, Japan

Tel : 029-887-1161 (ext. 7120) Fax : 029-887-1512 E-mail : kotake@tokyo-med.ac.jp

cranial nerve region. Furthermore, many reports have shown that it is also useful for the whole body with the progress of imaging device. However, since strong susceptibility artifacts occur due to air in the maxillary sinus in DWI of the orbital region, direct coronal images have not been used for diagnoses.

In the present study, coronal images were prepared by multiplanar reconstruction (MPR) for the MRI phantom, handmade phantom, and normal volunteers to compare with direct coronal images and to assess usefulness of MPR-coronal images in clinical cases.

Materials and methods

Subjects

Polyvinyl alcohol (PVA) gel phantom (Model 90-401, Nikko Fine Industries Co., Ltd., Tokyo, Japan) was used for the MRI phantom. Figure 1a shows the T1 weighted coronal image of the phantom. Three holders with a diameter of 19 mm to set sample containers are installed in the lower stand. PVA (Arabic Yamato, Yamato Co., Ltd., Tokyo, Japan), a low diffuse matter, was injected into the center. Air was injected at both the sides to simulate the maxillary sinus and we created conditions easily causing susceptibility artifacts.

A handmade phantom was made with 10 holes (diameters of 2 mm, 4 mm, 6 mm, 8 mm, and 10 mm, at a depth of 20 mm) on the upper and lower stand of the acrylic board. PVA was injected into the upper stand. Distilled water filled the lower stand, which was then sealed. It was put into a cistern to create conditions with little susceptibility artifact.

The purpose of the present study was explained to 10 healthy volunteers with no abnormal changes in visual performance (5 men and 5 women, ranging in age from 24 to 78). They were examined after obtaining their informed consent. Examinations were also performed on clinical cases of optic neuritis, orbital malignant lymphoma, and dysthyroid ophthalmopathy.

MR imaging

MR imaging was performed using a 1.5 T superconductive MR system (Avanto ; Siemens Medical Solutions, Erlangen, Germany). The maximum gradient strength was 45 mT/m. All MR images were obtained with a head matrix coil. Diffusion-weighted (DW) images were obtained using an echo planar imaging (EPI) sequence and short T1 inversion recovery (STIR) method, with b-values set at 0 and 1,000 sec/mm^2. Direct coronal DW images were obtained under the following parameters : 12000/180/74/10 (TR/TI/TE/excitations) ; echo train length 128 ; matrix 128 128 ; field of view (FOV) 300 mm ; acquisition time 8 min 12 sec. MPR-coronal DW images were also created using the data from transverse DW images with the following parameters : 11500/180/71/10 (TR/TI/TE/excitations) ; echo train length 128 ; matrix 128×128 ; FOV 300 mm ; acquisition time 7 min 52 sec. The slice thickness/gap was set to 2.3 mm/0 mm for both the methods to obtain isotropic data. No parallel imaging was used for the phantom experiments and healthy volunteers for the measurement of signal-to-noise ratio (SNR). However, parallel imaging was used for clinical cases to reduce artifacts and shorten the inspection time. We also used a special antisusceptibility device (Sat Pat ; Alliance Pharmaceutical, San Diego, CA, USA) that was placed on the orbit of normal volunteers and patients to reduce susceptibility artifacts.

Image analysis

The length of PVA of direct coronal DWI and MPR-coronal DWI was measured from the MRI phantom experiments. The distortion rate was obtained by the following equation :

$$\text{Percent distortion} = \frac{\text{true dimension (19 mm)} - \text{observed dimension}}{\text{true dimension (19 mm)}} \times 100$$

For the handmade phantom, seven slices of the apparent diffusion coefficient (ADC) map were prepared for direct coronal DWI and MPR-coronal DWI, respectively. We set the region of interest (ROI) in the center of the PVA (upper stage) and distilled water (lower stage) for each slice with a diameter of 10 mm, 8 mm, 6 mm, 4 mm, and 2 mm and measured the ADC value.

We set two points (e.g., frontal white matter and the globe) as ROI on the signal side and the background deviated from the head as ROI on the noise side based on the direct coronal DWI and MPR-coronal DWI of healthy volunteers, and then we calculated SNR.

The differences in ADC values and SNRs among direct coronal DWI and MPR-coronal DWI were analyzed using the Wilcoxon signed-ranks test. Values of $P<0.05$ were considered to indicate a statistically significant difference.

We also performed MPR-coronal DWI on clinical cases and measured ADC values of lesions.

Results

In the MRI phantom experiment, the PVA of direct coronal DWI was extended to 23.4 mm in the phase encoding direction. The distortion rate was as large as −23.2% (Fig. 1b). The length of PVA of MPR-coronal DWI was 18.8 mm. The distortion rate was 1.1%, which is within the allowable range (Fig. 1c).

We prepared seven slices of the ADC map (Fig. 2) from direct coronal DWI and MPR-coronal DWI, respectively in the handmade phantom experiment and measured the ADC values (Table 1). In the comparison of ADC values by diameter, the 2 mm diameter showed smaller values than diameters of 10 mm, 8 mm,

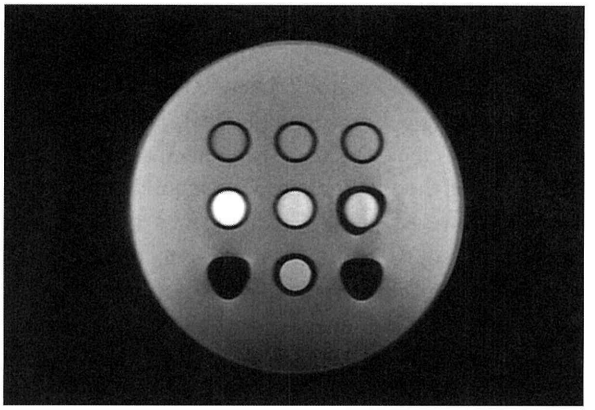

a

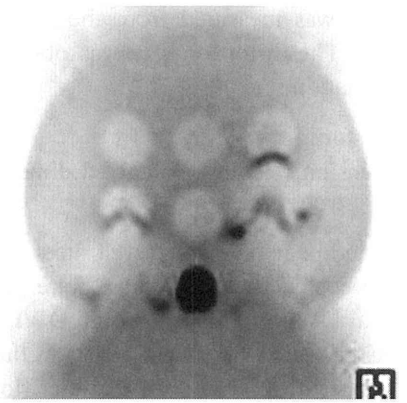

b

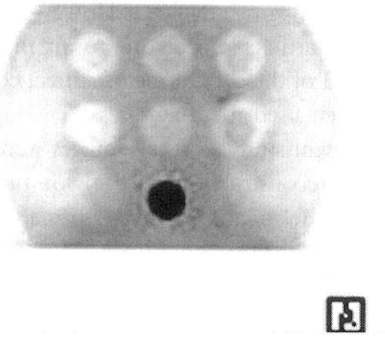

c

Fig. 1 Magnetic resonance imaging (MRI) phantom
a : T1 weighted coronal image
Polyvinyl alcohol (PVA) gel having different moisture content is sealed in the upper stand. PVA gel having different amount of Gd^{3+} is sealed in the middle stand. Three holders that can contain sample containers with an internal diameter of 19 mm are equipped in the lower stand. PVA (Arabic Yamato), a low diffuse matter, is filled into the center and air is injected to both sides to make an environment that can readily cause susceptibility artifact.
b : Direct coronal diffusion-weighted image (monochrome reverse imaging)
PVA was extended in the direction of phase encoding and the distortion rate was −23.2%.
c : Multiplanar reconstruction (MPR)-coronal diffusion-weighted image (monochrome reverse imaging)
The distortion rate was 1.1% and was within the allowable range.

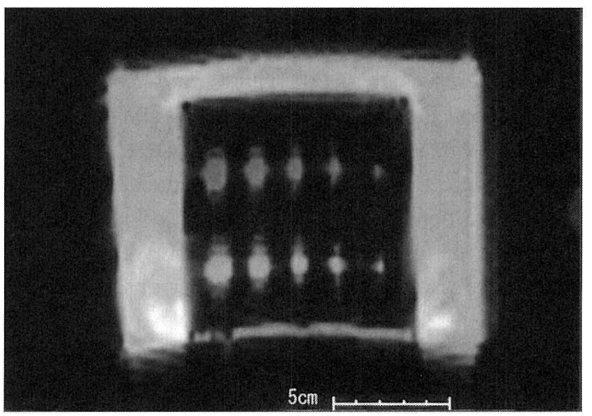

a

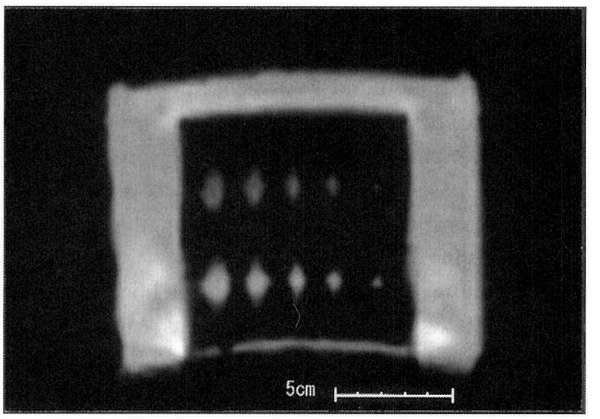

b

Fig. 2 Coronal apparent diffusion coefficient (ADC) map of handmade phantom
a : Direct coronal ADC map
b : MPR-coronal ADC map
The 2 mm diameter was too small for two maps, so visualization was poor and it was difficult to set region of interest (ROI).

6 mm, and 4 mm. This phenomenon may result from imprecise measurement of smaller diameters. In comparing the ADC values of PVA and distilled water by direct coronal DWI and MPR-coronal DWI, there was no significant difference for diameters of 10 mm, 8 mm, 6 mm, and 4 mm.

In the direct coronal DWI of volunteers, the temporal lobe base was extended in the phase encoding direction

Table 1 Comparison of mean ADC values between direct coronal DWI and MPR-coronal DWI

diameter	PVA		distilled water	
	direct	MPR	direct	MPR
10 mm	1.65±0.01	1.66±0.03	2.48±0.03	2.48±0.04
8 mm	1.64±0.01	1.66±0.03	2.47±0.03	2.43±0.04
6 mm	1.60±0.03	1.59±0.03	2.39±0.05	2.37±0.04
4 mm	1.56±0.07	1.56±0.04	2.34±0.04	2.32±0.03
2 mm	1.38±0.06	1.25±0.04	1.88±0.08	1.69±0.18

ADC value
Unit : $\times 10^{-3}$ mm^2/sec

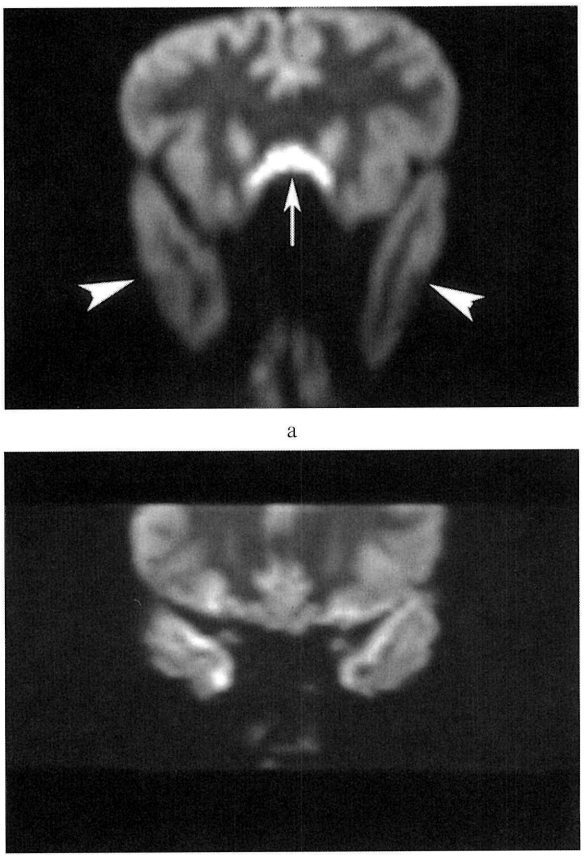

a

b

Fig. 3 Diffusion-weighted coronal image of volunteers
a : The temporal lobe base (white arrowhead) was extended in the direction of phase encoding and the image had strong distortions for direct coronal DWI. Artifact is observed in the cranial base visualized as high signal intensity (white arrow).
b : MPR-coronal DWI showed no distortion or artifact.

to create images with strong distortion (Fig. 3a). Meanwhile, the MPR-coronal DWI provided almost normal images (Fig. 3b). The average SNR of globe was 1.90±0.25 (mean±standard deviation) for direct coronal DWI and 1.78±0.25 for MPR-coronal DWI with no significant difference (P=0.092) between them. In addition, the average SNR of the white matter of the

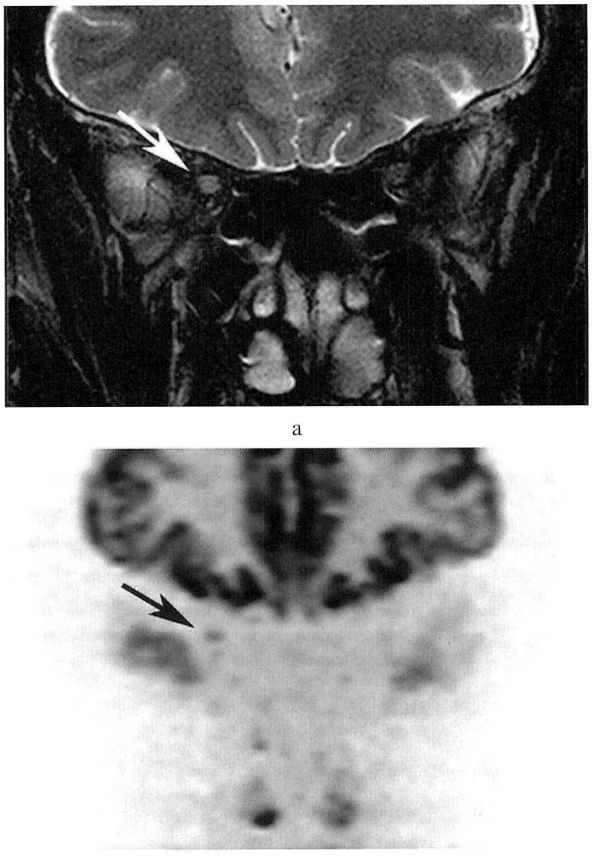

a

b

Fig. 4 Right acute optic neuritis (38-year-old man)
a : A high signal intensity is observed in the right optic nerve by Fat-suppressed T2 weighted coronal image (white arrow).
b : MPR-coronal DWI (the monochrome reverse imaging) also showed a high signal intensity (black arrow). ADC value was 0.89×10^{-3} mm^2/sec.

frontal lobe was 2.29±0.34 for direct coronal DWI and 2.30±0.27 for MPR-coronal DWI with no significant difference (P=0.878) between them.

We performed MPR-coronal DWI (monochrome reverse imaging) on cases of optic neuritis (Fig. 4), orbital malignant lymphoma (Fig. 5), and dysthyroid ophthalmopathy (Fig. 6) and obtained images without distortion. Lesions were visualized as areas with significant high signal intensity. We also measured ADC values from the MPR-coronal ADC map. The resulting values were 0.89×10^{-3} mm^2/sec for optic neuritis, 0.53×10^{-3} mm^2/sec for orbital malignant lymphoma and 1.34×10^{-3} mm^2/sec for dysthyroid ophthalmopathy.

Discussion

DWI is mainly used for the cranial nerve region to detect acute phase cerebrovascular accidents, for which DWI usefulness has been established. However, in the craniocervical region, it has been difficult to obtain

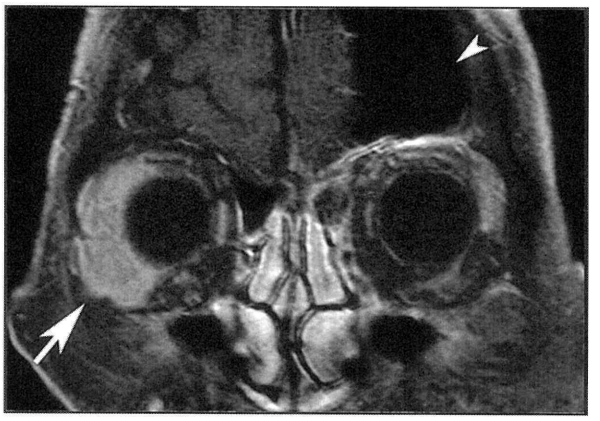

a

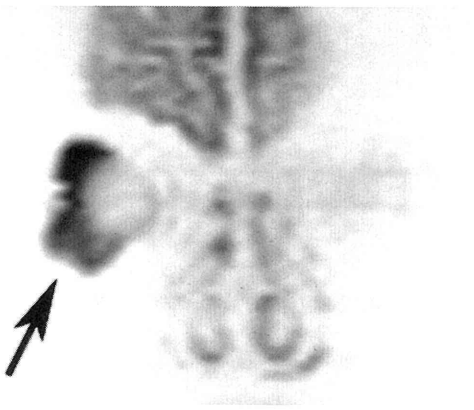

b

Fig. 5 Orbital malignant lymphoma (85-year-old man)
a : Gadolinium-enhanced fat-suppressed T1 weighted image shows a tumor-like mass continued to the lacrimal gland at the outer side of the right globe (white arrow). The tumor is evenly enhanced and the displacement of the globe is slight. Postoperative changes of chronic subdural hematoma are observed in the left frontal lobe (white arrowhead).
b : MPR-coronal DWI (the monochrome reverse imaging) shows a strong high signal intensity (black arrow). ADC value is only 0.53×10^{-3} mm²/sec.

a

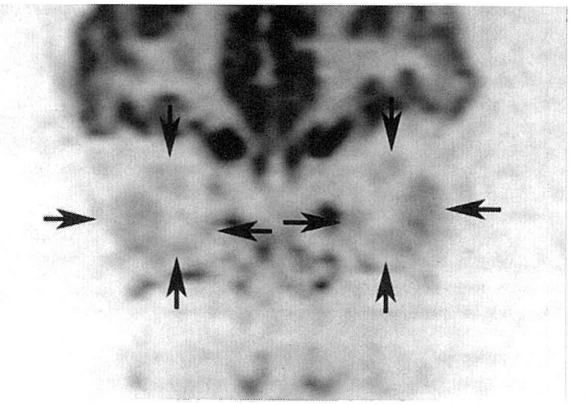

b

Fig. 6 Dysthyroid ophthalmopathy (48-year-old woman)
a : Fat-suppressed T2 weighted coronal image shows that the bilateral extraocular muscles are all thickened indicating a high signal intensity (white arrow).
b : MPR-coronal DWI (monochrome reverse imaging) shows a faintly high signal intensity (black arrow). The ADC value is 1.34×10^{-3} mm²/sec.

images for evaluation of clinical cases due to image distortion caused by susceptibility artifacts. DWI in the abdominal region with accompanying strong susceptibility artifacts was obtained by improving the echo-planar technique and its clinical usefulness has been reported[1)2)]. Wang et al.[3)] was the first to report DWI in the craniocervical region. They performed transverse DWI on 97 patients. However, they could not measure the ADC values due to the presence of susceptibility artifacts, which are characteristic of EPI caused by air in paranasal sinuses. They reported that they had no choice but to exclude 16 patients from their study. After Wang et al.[3)], several authors[4)–6)] reported DWI in the craniocervical region. However, all of them are transverse images and no DWI in the coronal section has been performed.

A new technology called line scan DWI was developed to eliminate susceptibility artifacts. The line scan DWI does not requires any special hardware and artifacts due to movement do not affect the entire image. Therefore, it has the advantage of eliminating artifacts due to movement[7)]. For line scan DWI of the craniocervical region, the effect of image deterioration caused by susceptibility artifact is dramatically reduced as compared to EPI-DWI in patients with metals such as artificial dentures and lesions near paranasal sinuses[8)]. The line scan DWI is excellent for low- and middle-field MR system for which the EPI method is technologically disadvantageous and for regions in which the effect of susceptibility artifact is strong. However, EPI-DWI is preferred because it has a short acquisition time. In addition, the line scan DWI cannot be used by the MRI machine at our institute and, at present, there are few models that can use the line scan DWI.

The direct coronal DWI in the orbital region has not been used in clinical cases because of the strong suscepti-

bility artifact caused by air in the maxillary sinus. However, coronal images are required for diagnosing the orbital region. Therefore, high-quality coronal DWI is essential. In the present study, we took transverse images with an appropriate slice thickness for obtaining isotropic data and prepared MPR-coronal DWI, and compared it to the direct coronal DWI. The isotropic imaging is an imaging technology that equalizes the spatial resolution in all directions[9]. The slice thickness for the isotropic imaging is 2.3 mm under FOV 300 mm and matrix 128×128 in the MRI machine at our institute. The acquisition time was long, due to the thin slice (i.e., direct coronal DWI : 8 min 12 sec, MPR-coronal DWI : 7 min 52 sec). However, the time was shortened to 4 min 57 sec for MPR-coronal DWI in the clinical cases using parallel imaging.

In the experiment under a large effect of susceptibility artifact using MRI phantom, the distortion was extended in the direction of the phase encoding by direct coronal DWI. Images of healthy volunteers also had strong distortion and it was, therefore, difficult to use for diagnosis. Meanwhile, the distortion rate of MPR-coronal DWI was 1.1% and was within ±5% of the allowable range proposed by the Nuclear Magnetic Resonance Committee, American Association of Physicists in Medicine[10].

Human tissues can be roughly divided into cells and intercellular space, and the diffusion contrast of DWI mainly depends on water molecules in the intercellular space. The cells in a malignant tumor are increased in number or enlarged, narrowing the intercellular space and restricting water molecule diffusion, and are observed as an abnormal signal[11]. Sugahara et al.[12] and Guo et al.[13] reported that the results of comparisons of the ADC values and histopathologic findings strongly suggested that greater cellularity is associated with more restricted diffusion. Measurements of ADC values are advantageous because there is no effect by T2-weighted imaging compared to DWI and analyses of diseases are possible quantitatively. Thus, precise measurements of ADC values are required. In the direct coronal DWI of volunteers, the temporal lobe base is extended in the direction of phase encoding and has strong distortion. We surmised that we could not measure ADC values precisely.

In the handmade phantom experiment under little susceptibility artifact, the average ADC value obtained by the ADC map of the direct coronal DWI and MPR-coronal DWI had no significant difference other than for 2 mm diameter. As a result, we considered that there was no problem for measuring ADC values by MPR-coronal ADC map. The ADC value for 2 mm showed a significant difference because it was too small to measure (a portion of the setting for ROI deviated from the target).

There was no significant difference in average SNR of globes and the white matter of the frontal lobe of volunteers between the direct coronal DWI and MPR-coronal DWI. Therefore, it was supposed that the MPR method would not degrade SNR.

The number of clinical cases is small. However, high-quality images without distortion were obtained by MPR-coronal DWI in all cases. Lesions were visualized as high signal intensity. Figure 5 is an acute optic neuritis related to multiple sclerosis. ADC value was 0.89×10^{-3} mm^2/sec. Hickman et al.[14] reported that the ADC value of an old optic neuritis (one year or more elapsed from onset) was 1.32×10^{-3} mm^2/sec and it was significantly higher than 0.99×10^{-3} mm^2/sec of a normal optic nerve. We searched reports for ADC values of acute optic neuritis but we could not find them. However, it is reported that active lesions enhanced evenly by contrast-enhanced T1 weighted imaging in multiple sclerosis in the brain was reduced to 0.77×10^{-3} mm^2/sec[15]. Also for acute optic neuritis, the ADC value was reduced compared with the normal optic nerve. It was supposed that it might be used to quantitatively judge the effectiveness of therapy by measuring ADC values after treatment.

In Figure 6, the ADC value of orbital malignant lymphoma is only 0.53×10^{-3} mm^2/sec. It has been reported that the entire tumor is visualized as a high signal intensity by DWI because malignant lymphoma in the brain has a higher cell density[16]. The ADC value is reduced significantly to 0.58×10^{-3} mm^2/sec and can be distinguished from gliomas and metastasis[17]. Also in the craniocervical region, it has been reported that the ADC value of malignant lymphoma was only 0.66×10^{-3} mm^2/sec and can be distinguished from carcinoma (1.13×10^{-3} mm^2/sec) and benign solid tumor (1.56×10^{-3} mm^2/sec)[3]. In the present study, orbital malignant lymphoma showed ADC values as low as malignant lymphoma in the brain and the craniocervical resion.

In the future, the setting of the specific ADC value of each orbital disease may become possible by increasing the number of cases. We expect to distinguish malignant lymphoma from other neoplastic lesions of the orbit by measuring ADC values. In particular, if malignant lymphoma can be distinguished from lymphoproliferative diseases, including reactive lymphoid hyperplasia and atypical lymphoid hyperplasia that are hard to be distinguished by conventional MRI, then the clinical significance will be high.

Conclusion

1. Direct coronal DWI showed significantly strong distortions of images in the phantom experiment

under large effect of susceptibility artifact and for the orbit of volunteers. The distortion of images was negligibly small by MPR-coronal DWI.

2. In the phantom experiment with little effect of susceptibility artifact, there was no significant difference in ADC value between direct coronal DWI and MPR-coronal DWI. It was estimated that the MPR-coronal ADC map might be used for measuring ADC values.
3. There was no significant difference in SNR by MPR-coronal DWI compared to direct coronal DWI. Image processing did not degrade SNR.

References

1) Yamashita Y, Namimoto T, Mitsuzaki K, Urata J, Tsuchigame T, Takahashi M, Ogawa M : Mucin-producing tumor of the pancreas : diagnostic value of diffusion-weighted echo-planar MR imaging. Radiology **208** : 605-609, 1998
2) Kim T, Murakami T, Takahashi S, Hori M, Tsuda K, Nakamura H : Diffusion-weighted single-shot echoplanar MR imaging for liver disease. AJR **173** : 393-398, 1999
3) Wang J, Takashima S, Takayama F, Kawakami S, Saito A, Matsushita T, Momose M, Ishiyama T : Head and neck lesions : characterization with diffusion-weighed echo-planar MR imaging. Radiology **220** : 621-630, 2001
4) Yoshino N, Yamada I, Ohbayashi N, Honda E, Ida M, Kurabayashi T, Maruyama K, Sasaki T : Salivary glands and lesions ; evaluation of apparent diffusion coefficients with aplit-echo diffusion-weighted MR imaging-initial results. Radiology **221** : 837-842, 2001
5) Sumi M, Takagi Y, Uetani M, Morikawa M, Hayashi K, Kobasawa H, Aikawa K, Nakamura T : Diffusion-weighted echoplanar MR imaging of the salivary glands. AJR **178** : 959-965, 2002
6) Sumi M, Sakihama N, Sumi T, Morikawa M, Uetani M, Kabasawa H, Shigeno K, Hayashi K, Takahashi H, Nakamura T : Discrimination of metastatic cervical lymph nodes with diffusion-weighted MR imaging in patients with head and neck cancer. Am J Neuroradiol **24** : 1627-1634, 2003
7) Maier SE, Gudbjartsson H, Patz S, Hsu L, Lovblad K, Edelman RR, Warach S, Jolesz FA : Line scan diffusion imaging ; characterization in healthy subjects and stroke patients. AJR **171** : 85-93, 1998
8) Maeda M, Kato H, Sakuma H, Maier SE, Takeda K : Usefulness of the apparent diffusion coefficient in line scan diffusion-weighted imaging for distinguishing between squamous cell carcinomas and malignant lymphomas of the head and neck. Am J Neuroradiol **26** : 1186-1192, 2005
9) Kalender WA : Thin-section three-dimensional spiral CT ; Is isotropic imaging possible ? Radiology **197** : 578-580, 1995
10) Price RR, Axel L, Morgan T, Newman R, Perman W, Schneiders N, Selikson M, Wood ML, Thomas SR : Quality assurance methods and phantoms for magnetic resonance imaging ; Report of AAPM nuclear magnetic resonance Task Group No. 1. Med Phys **17** : 287-295, 1990
11) Lyng H, Haraldseth O, Rofstad EK : Measurement of cell density and necrotic fraction in human melanoma xenografts by diffusion weighted magnetic resonance imaging. Magn Reson Med **43** : 828-836, 2000
12) Sugahara T, Korogi Y, Kochi M, Ikushima I, Shigematu Y, Hirai T, Okuda T, Liang L, Ge Y, Komohara Y, Ushio Y, Takahashi M : Usefulness of diffusion-weighted MRI with echo-planar technique in the evaluation of cellularity in gliomas. J Magn Reson Imaging **9** : 53-60, 1999
13) Guo AC, Cummings TJ, Dash RC, Provenzale JM : Lymphomas and high-grade astrocytomas ; comparison of water diffusibility and histologic characteristics. Radiology **224** : 177-183, 2002
14) Hickman SJ, Wheeler-Kingshott CAM, Jones J, Miszkiel KA, Barker GJ, Plant GT, Miller DH : Optic nerve diffusion measurement from diffusion-weighted imaging in optic neuritis. Am J Neuroradiol **26** : 951-956, 2005
15) Roychowdhury S, Maldjian JA, Grossman RI : Multiple sclerosis ; comparison of trace apparent diffusion coefficients with MR enhancement pattern of lesion. Am J Neuroradiol **21** : 869-874, 2000
16) Okamoto K, Ito J, Ishikawa K, Sakai K, Tokiguchi S : Diffusion-weighted echo-planar MR imaging in differential diagnosis of brain tumors and tumor-like conditions. Eur Radiol **10** : 1342-1350, 2000
17) Stadnik TW, Chaskis C, Michotte A, Shabana WM, Rompaey KV, Luypaert R, Budinsky L, Jellus V, Osteaux M : Diffusion-weighted MR imaging of intracerebral masses ; comparison with conventional MR imaging and histologic findings. Am J Neuroradiol **22** : 969-976, 2001

眼窩領域の拡散強調画像：直接冠状断像と多断面再構成画像による冠状断像の比較検討

小竹文雄　森本恵爾　小槻泰三
新井元

東京医科大学霞ヶ浦病院放射線科

眼窩領域の拡散強調画像は下方に上顎洞の空気があるため磁化率アーチファクトが強く出現し、直接冠状断像は診断に用いられなかった。今回、MRI用ファントムと自作ファントムおよび正常ボランティアに対し多断面再構成画像（MPR）による冠状断像を作製し、直接冠状断像と比較した。また、臨床症例に対する有用性についても検証した。

磁化率アーチファクトの影響が大きい環境下でのMRI用ファントム実験では直接拡散強調冠状断像の歪み率は−23.2%で強い歪みが認められたが、MPRによる拡散強調冠状断像の歪み率は1.1%と許容範囲であった。磁化率アーチファクトの影響の少ない環境下での自作ファントム実験では見かけの拡散係数（ADC）値は直接拡散強調冠状断像とMPRによる拡散強調冠状断像で有意差はなく、ADC値計測にMPRによる冠状断のADCマップを用いることが可能と考えられた。ボランティアの眼球の平均信号雑音比（SNR）は直接拡散強調冠状断像で1.90±0.25（平均値±標準偏差）、MPRによる拡散強調冠状断像では1.78±0.25で有意差はなかった（$P=0.092$）。また、前頭葉白質の平均SNRも直接拡散強調冠状断像で2.29±0.34、MPRによる拡散強調冠状断像では2.30±0.27で有意差はなかった（$P=0.878$）。

視神経炎や眼窩悪性リンパ腫および甲状腺眼症の症例にMPRによる拡散強調冠状断像（白黒反転表示）を施行した結果、歪みのない画像が得られ、病変部は明瞭な高信号として描出された。

以上の実験結果や臨床研究により眼窩領域では直接拡散強調冠状断像よりMPRによる拡散強調冠状断像が画像が良好で、ADC測定やSNRにも支障がないことから臨床症例にも使用可能と考えられた。

〈キーワード〉 眼窩、MRI、拡散強調画像、多断面再構成画像、 等方性画像